High-temperature series expansions for Ising-like systems on fractals

Fábio D. A. Aarão Reis and R. Riera
Departamento de Física, Pontifícia Universidade Católica do Rio de Janeiro, Caixa Postal 38071, 22452-970 Rio de Janeiro, Rio de Janeiro, Brazil
(Received 5 April 1993; revised manuscript received 24 September 1993)

High-temperature series expansions up to 16th order for the Ising model susceptibility and for the second moment of the correlation function are generated for fractal lattices of the Sierpinski carpet family. The critical temperature and the critical exponents γ and ν are obtained from the series analysis method of differential approximants. From our results, we test the validity of estimates previously obtained in the literature and examine the effect of lacunarity on γ and ν. For carpets with the same fractal dimension, we found that ν decreases as lacunarity decreases.

PACS number(s): 05.50.+q, 64.60.Ak, 75.10.Hk

I. INTRODUCTION

The phase transitions of spin systems on nontrivial self-similar fractal lattices have been mostly studied for the Sierpinski carpet family [1] by real-space renormalization-group (RG) [2–5] methods and numerical simulations [6,7]. In the RG techniques, the rescaling factor cannot be smaller than the lattice self-similar factor, which implies the use of large cells for some fractals. In these cases, calculations cannot be performed in practice unless drastic approximations are done, such as bond moving, on the lattice structure. Analogously, when the lattice self-similar factor increases, the numerical simulations are possible only for the very first stages of the lattice construction, giving less reliable results due to finite-size effects. Consequently, these approaches do not allow a complete study of universality classes of statistical systems on fractals.

Recently, methods for computing the number of embeddings of graphs in self-similar structures were proposed [8,9], allowing the use of the series-expansion technique for statistical systems on these geometries. In comparison to other techniques, the series-expansion method provides the most reliable results whose accuracy can be improved in a systematic way by increasing the order of the series [10].

The graph counting method proposed by the authors [9] can be used in a fairly general family of self-similar deterministic fractals which are obtained by the iteration of a fixed rule of construction. It enables one to obtain the behavior of statistical systems on fractal lattices which have the same fractal dimension but different lacunarities [1], allowing a complete study of those system on non-Euclidean lattices. In this paper, we apply the graph counting method shown in [9] to find the coefficients of the high-temperature series expansions for the susceptibility and for the second moment of the correlation function of the Ising model on Sierpinski carpets.

The setup of this article is the following. In Sec. II we present the Sierpinski carpets and recall the attainment of the high-temperature series expansions for the Ising model susceptibility and the second moment of the correlation function. We also present our numerical calculations of the coefficients of the series. In Sec. III we briefly recall the series analysis method of differential approximants and present the results for the critical temperature T_c and critical exponents γ and ν. Section IV comprises comparisons with other existing data, discussions, and analysis.

II. NUMERICAL CALCULATIONS

The Sierpinski carpets are characterized by two integer numbers b and m. An initial unit square is divided into b^2 subsquares from which m are discarded forming m lacunas. Such initiator pattern replaces each of the remaining b^2-m subsquares and the lattice is rescaled by a factor b in order that the smallest subsquares be of unit area. The fractal is obtained by repeating this operation indefinitely. At each stage, Ising spins are located at the corners of the elementary squares.

Here we consider carpets characterized by a symmetric distribution of lacunas. For $m=1$, the lacuna is at the center of the initiator; for $m>1$, either the lacunas are joined at the center of the initiator or they are spread out symmetrically, generating lattices with the same fractal dimension $[D_f=\ln(b^2-m)/\ln b]$ but different lacunarities [1] (see Fig. 1).

High-temperature series expansions of the Ising model correlation function in zero field are obtained in a standard way by writing the single-bond Boltzmann factor $\exp(\beta J S_i S_j)$ as $\cosh(\beta J)[1+v S_i S_j]$ and expanding all products [11]. The result is ($\beta=1/k_B T$ and $v=\tanh\beta J$)

$$\Gamma^{(i)}(r,v)=\langle S_i S_{i+r}\rangle=\sum_{n=1}^{\infty} q_n^{(i)}(r) v^n , \tag{1a}$$

with $q_n^{(i)}(r)$ obtained from the number of graphs with n bonds having two end points in a distance r apart (made up by n-step self-avoiding walks plus contributions from shorter chains with polygons) starting at site i. Note that in a fractal lattice, the sites are not all equivalent (see Fig. 1). Hence the correlation function defined in (1a) depends

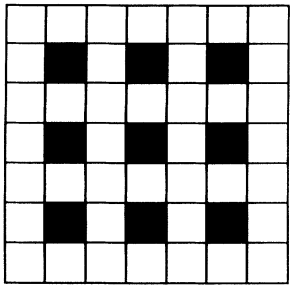

(a)

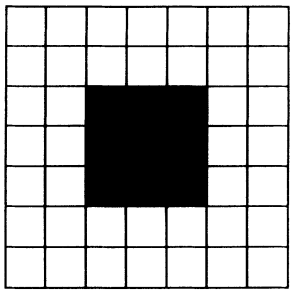

(b)

FIG. 1. Initiators of Sierpinski carpets characterized by parameters $b=7$ and $m=9$: (a) high lacunarity and (b) low lacunarity.

on the root site i.

We then consider the average correlation function defined as

$$\Gamma(r,v)=\frac{1}{N}\sum_{i=1}^{N}\Gamma^{(i)}(r,v)\ , \tag{1b}$$

with N the total number of sites. Using (1a), it can be written as

$$\Gamma(r,v)=\sum_{n=1}^{\infty}q_n(r)v^n\ , \tag{1c}$$

with $q_n(r)=(1/N)\sum_{i=1}^{N}q_n^{(i)}(r)$, the average number of graphs with n bonds having any initial site i and two end points in a distance r apart. The moments of the correlation function $\Gamma(r,v)$ may be formally defined by

$$\mu_p(v)=\sum_{r\neq 0}r^p\Gamma(r,v)=\sum_{r\neq 0}\sum_{n=1}^{\infty}q_n(r)r^pv^n\ . \tag{2}$$

Using (1), the fluctuation theorem for the reduced susceptibility per spin then reads

$$\chi/\beta N=\frac{1}{N}\sum_{r}\sum_{i}\langle S_iS_{i+r}\rangle=1+\sum_{r\neq 0}\Gamma(r,v)=1+\mu_0(v) \tag{3a}$$

or

$$\chi/\beta N=1+\sum_{n=1}^{\infty}d_nv^n\ , \tag{3b}$$

with d_n obtained from the total number of graphs with n bonds having any initial site i and two end points at any distance apart divided by the total number of sites. Similarly, the second moment of the correlation function is given by

$$\mu_2(v)=\sum_{n=1}^{\infty}\rho_nv^n\ , \tag{4}$$

with ρ_n –the total number of chains and chains plus polygon configurations per site in which each chain is weighted by the square of its end-to-end distance. Formally, from Eq. (2)

$$\rho_n=\sum_{r}q_n(r)r^2\equiv\langle R_n^2\rangle d_n\ , \tag{5}$$

where $\langle R_n^2\rangle$ is the mean square size of the nth-order distribution.

We also analyze the series

$$S(v)=\sum_{n=1}^{\infty}\langle R_n^2\rangle v^n\ . \tag{6}$$

It is expected for Euclidean lattices that functions (3) and (4) have the critical behavior $F(v)\sim(1-v/v_c)^{-\theta}$ for $v\to v_c^-$, with critical exponent θ equal to γ and $\gamma+2\nu$, respectively [12]. The sequence of coefficients $\langle R_n^2\rangle$ defined in (6) is analogous to the mean square size of a self-avoiding walk of n steps. The series (6) has an exact critical parameter $v_c=1$ and critical exponent $\theta=1+2\nu$ [13].

In what follows we assume that the above critical behavior for functions (3), (4), and (6) also holds for Ising systems on regular or deterministic fractals for which the unit generator is a composition of basic plaquettes of the standard lattices as squares, cubes, triangles, etc. In order to calculate the coefficients of series (3) and (4) we have to proceed with the enumeration of all the connected graphs that contribute to each order of these series and their respective weights (they are the same as in the square lattice). As we are not dealing with translationally invariant lattices, methods based on the enumeration of only star graphs [11] cannot be used.

We have performed the series expansions of the functions (3) and (4) up to 16th order for several Sierpinski carpets using the exact graph counting method shown in [9]. In the Appendix we give details of the method and its application for the graph of Fig. 2 on the carpet with

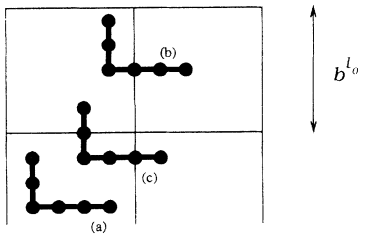

FIG. 2. Schematic representation of four neighboring l_0-stage reproduction of the fractal lattice with contributions to (a) $G(l_0)$, (b) $H_1(l_0)$, and (c) $H_2(l_0)$.

TABLE I. Coefficients d_n, $1 \le n \le 16$, of the Ising magnetic susceptibility high-temperature expansion [Eq. (3)] for carpets characterized by parameters (b,m). For $m=9$, the superscripts l and h stand for lattices with low and high lacunarity, respectively (see text).

(b,m)	(5,1)	$(7,9)^l$	$(7,9)^h$	(3,1)
n				
1	115/29	182/47	117/31	42/11
2	342/29	528/47	330/31	120/11
3	48 893/1392	30 807/940	1871/62	1379/44
4	22 461/232	41 501/470	97 519/1240	1825/22
5	369 097/1392	222 123/940	503 483/2480	76 649/352
6	245 425/348	144 083/235	627 907/1240	48 673/88
7	62 278 037/33 408	371 173/235	3 102 019/2480	490 461/352
8	8 998 823/1856	187 884/47	7 514 621/2480	1 213 117/352
9	69 824 299/5568	377 712 163/37 600	3 608 677/496	2 977 469/352
10	29 819 689/928	234 703 981/9400	42 840 053/2480	7 229 507/352
11	304 253 013/3712	2 318 676 343/37 600	100 972 047/2480	139 514 117/2816
12	2 313 615 641/11 136	1 420 352 147/9400	2 953 154/31	20 878 335/176
13	4 382 998 903/8352	13 850 652 619/37 600	549 910 771/2480	198 946 397/704
14	44 079 089 749/33 408	8 391 861 501/9400	636 917 751/1240	85 700 857/128
15	110 518 479 585/33 408	81 037 693 701/37 600	2 940 660 387/2480	4 448 917 749/2816
16	276 115 149 487/33 408	194 783 590 201/37 600	135 382 151 133/49 600	5 227 596 829/1408

$b=3$ and $m=1$. We also show in the Appendix an explicit derivation of the first two terms of series (3b) and (4) for the same carpet. Tables I and II show the coefficients d_n and ρ_n for some carpets. Coefficients $\langle R_n^2 \rangle$ of series (6) were obtained using (5).

III. SERIES ANALYSIS AND RESULTS

Series (3) and (6) were analyzed using the method of differential approximants of the first and second order [14] to obtain the critical exponents $\theta=\gamma$ and $1+2\nu$, respectively. In brief, this method is based on fitting the series coefficients of a function $F(v)$ to the polynomial coefficients of a Kth-order differential equation whose solution gives an approximate representation of the function. By choosing the appropriate degree K, the approximants provide a representation of different singular structures of the function.

We have worked with the nonhomogeneous first- and second-order differential equations

$$Q_0(v)F(v)+Q_1(v)D_vF(v)=P(v)\ , \tag{7a}$$

$$Q_0(v)F(v)+Q_1(v)D_vF(v)+Q_2(v)D_v^2F(v)=P(v)\ , \tag{7b}$$

with $D_v \equiv v(d/dv)$ and $Q_0(v)$, $Q_1(v)$, $Q_2(v)$, and $P(v)$ polynomials of order M_0, M_1, M_2, and L respectively. The singular behavior of the approximants $F(v)$ can be determined by applying standard techniques from theory of

TABLE II. Coefficients ρ_n, $1 \le n \le 16$, of the high-temperature expansion of the second moment of the Ising correlation function [Eq. (4)] for carpets characterized by parameters (b,m). For $m=9$, the superscripts l and h stand for lattices with low and high lacunarity, respectively (see text).

(b,m)	(5,1)	$(7,9)^l$	$(7,9)^h$	(3,1)
n				
1	115/29	182/47	117/31	42/11
2	912/29	1408/47	880/31	320/11
3	222 461/1392	139 607/940	8463/62	6243/44
4	236 833/348	29 023/47	85 128/155	6375/11
5	1 205 051/464	432 391/188	4 901 027/2480	745 617/352
6	12 841 312/1392	1 872 456/235	4 096 257/620	316 637/44
7	1 038 885 773/33 408	6 150 221/235	51 889 059/2480	8 159 053/352
8	841 690 613/8352	3 879 922/47	19 729 409/310	6 311 913/88
9	5 287 410 797/16 704	9 477 325 619/37 600	464 905 753/2480	75 642 837/352
10	2 699 096 677/2784	880 660 951/1175	667 026 461/1240	110 407 917/176
11	97 146 334 717/33 408	16 392 514 403/7520	3 744 402 847/2480	5 045 625 445/2816
12	11 928 904 249/1392	29 249 117 829/4700	2 579 233 369/620	884 335 631/176
13	207 771 943 123/8352	657 612 748 507/37 600	27 988 590 747/2480	9 765 095 843/704
14	1 190 667 332 103/16 704	45 587 440 029/940	3 744 625 871/124	26 588 477 521/704
15	6 745 843 778 961/33 408	624 791 833 613/4700	198 093 686 603/2480	286 102 960 197/2816
16	1 182 392 573 428/2088	847 622 020 411/2350	1 295 946 634 486/6200	95 175 853 745/352

differential equations to (7). In the case of the first-order differential equation (7a) the critical point v_c is obtained from the root of polynomial $Q_1(v)$ and the approximants $F_{\{M_0,M_1,L\}}(v)$ represent functions of the form [14]

$$F(v)\sim A(v)+B(v)|v-v_c|^{-\theta} \quad (v\to v_c) , \tag{8}$$

where $A(v)$ and $B(v)$ are analytic at v_c and [14] $\theta=-Q_0(v_c)/v_cQ_1'(v_c)$.

In the case of the second-order differential equation (7b), the critical point v_c is obtained by the root(s) of polynomial $Q_2(v)$. Simple zeros in $Q_2(v)$ indicate a solution of the form (8) with [14] $\theta=1-Q_1(v_c)/v_cQ_2'(v_c)$. Double roots or closely spaced zeros in $Q_2(v)$ indicate that the approximants $F_{\{M_0,M_1,M_2,L\}}(v)$ represent functions with confluent singularities [14]

$$F(v)=B(v)|v-v_c|^{-\theta}+C(v)|v-v_c|^{-\theta'}+A(v) , \tag{9a}$$

where $A(v)$, $B(v)$, and $C(v)$ are analytic at v_c, $\theta>\theta'$, and $\Delta=\theta-\theta'\neq$integer. Equation (9a) can be rewritten as

$$F(v)=A(v)+B(v)|v-v_c|^{-\theta} \times\{1+[C(v)/B(v)]|v-v_c|^{\Delta}\} . \tag{9b}$$

For the two-dimensional (2D) Ising model, thermodynamic quantities such as the magnetic susceptibility behave close to the critical point like (9b), but with the correction-to-scaling exponent $\Delta=1$. This corresponds to an analytic correction and, in fact, such behavior is included in the form (8). Such analytic correction to scaling for planar Ising models may arise from nonlinear thermal and ordering fields [15]. On the other hand, for the 3D Ising model it is believed that the thermodynamic quantities present nonanalytic corrections to scaling ($\Delta\neq$integer). Accordingly, one should also examine expressions for the model on fractals of the form (9). In principle, such forms can result from second-order differential approximants, as mentioned, with the requisite double roots of $Q_2(v)$.

In the analysis of the second-order differential approximants, however, we find that the form (8) holds for almost all the approximants for our series. While this finding is consistent with an integer correction to scaling exponent Δ in (9b), it may also be due to a weak confluent term as compared with the leading term, which is numerically represented by an analytic term as well. The attainment of an isolated root of $Q_2(v)$ may also represent some "optimal" choice of critical point and effective exponent by the approximants. Further studies using special techniques, e.g., imposing double roots of $Q_2(v)$ or constructing a new function from $F(v)$ in which the leading singular term is canceled out [16] (the residual critical exponent estimates from the analysis of differential approximants for this new function should, in principle, represent the correction-to-scaling exponent), would be needed to detect nonanalytic confluent terms if they exist.

We present the estimates of v_c and θ in (8) from first- and second-order approximants. The presence of the analytic part $A(v)$ is such that usual D log Padé approximants, which are best suited for functions with strong isolated power-law singularities [$A(z)=0$ in (8)], do not show satisfactory convergence properties, at least up to the order of the series studied.

Using the leading $N+1$ ($13\le N\le 16$) coefficients of the 16th-order series expansions of functions (3) and (6), we search for a set of approximants $F_{\{M_0,M_1,L\}}(v)$ in (7a) and $F_{\{M_0,M_1,M_2,L\}}(v)$ in (7b), where L runs from 1 to 8; M_0, M_1, and $M_2\ge 2$; and $|M_0-M_1|$, $|M_1-M_2|$, and $|M_2-M_0|=0$ or 1 (diagonal and near diagonal approximants) [13].

The estimates of v_c and θ for each leading order N are obtained by taking means of the estimates of critical parameters with an error bar that is twice the standard deviation. Defective approximants or those which lie well outside the scatter of the remaining ones are discarded.

In order to appreciate the convergence properties of the approximants, in Tables III and IV we show, respectively, the estimates of the critical parameter v_c and exponent γ obtained from the Ising magnetic susceptibility series (3) and exponent $2\nu+1$ obtained from series (6) at the critical parameter $v_c=1$ for the carpet with $b=3$ and $m=1$. We also show, for both first- and second-order approximants, the number l_c of calculated approximants, the number l_d of defective approximants, and the number l_n of approximants used in calculating the mean for each fixed value of N.

From the estimates for each N, the final estimate is obtained by considering at least three superimposed values within the error bars. This procedure captures the convergence properties of the series and when applied to the series of the square lattice provides final estimates that include the exact results.

Our final estimates are shown in Table V. The $K=1$ and 2 differential approximants (8) show similar convergence. The exponent ν of the second lattice shown in Table V deserves a special comment. The $K=1$ approximants give estimates around 1.0, which is the value of the square lattice. The $K=2$ approximants give almost

TABLE III. Estimates of critical parameter v_c ($v_c=\tanh J/k_BT_c$) and exponent γ obtained from $K=1$ and 2 approximants for the carpet with $b=3$ and $m=1$ according to the leading order N of the series expansion. Also shown is the number of approximants that were calculated (l_c), defective (l_d), and used in calculating the mean (l_n) for each N.

N	l_c	l_d	l_n	v_c	γ
			$K=1$ approximants		
12	10	7	3	0.4562±0.0014	2.28±0.06
13	12	3	8	0.4556±0.0007	2.25±0.09
14	12	4	8	0.4556±0.0007	2.24±0.05
15	12	8	3	0.4563±0.0037	2.23±0.04
			$K=2$ approximants		
12	8	3	5	0.4548±0.0045	2.22±0.17
13	11	2	7	0.4561±0.0003	2.27±0.02
14	14	5	9	0.4555±0.0006	2.24±0.04
15	15	7	7	0.4549±0.0017	2.20±0.16
16	18	14	3	0.4560±0.0023	2.28±0.16

TABLE IV. Estimates of exponent $2\nu+1$ obtained from $K=1$ and 2 approximants for the carpet with $b=3$ and $m=1$ according to the leading order N of the series expansion. Also shown is the number of approximants that were calculated (l_c), defective (l_d), and used in calculating the mean (l_n) for each N.

N	l_c	l_d	l_n	$2\nu+1$
		$K=1$ approximants		
12	10	2	8	3.7±1.4
13	12	3	9	3.82±0.39
14	12	0	10	3.81±0.12
15	12	0	11	3.71±0.45
16	12	0	10	3.55±0.19
		$K=2$ approximants		
12	8	2	5	3.3±0.9
13	11	2	9	3.4±1.3
14	14	2	11	3.93±0.37
15	15	9	4	3.60±0.41
16	18	10	6	3.54±0.14

100% of the estimates less than 1.0, with two regions of convergence, corresponding to high and low order L of the polynomial $P(v)$ in (7b); this is responsible for the large error bar. As these two regions are less than one, this is a strong support for $\nu<\nu(D=2)$.

IV. ANALYSIS AND CONCLUSIONS

From Table V, our estimates confirm the expected result $T_c<T_c(D=2)$ and the general trend previously obtained $\gamma>\gamma(D=2)$. On the other hand, the trend $\nu>\nu(D=2)$ obtained in previous works [5–7] that dealt only with carpets with central lacunas is not confirmed here.

Our method of graph counting allows the derivation of the exact series expansions also for carpets with no central lacunas and then it is possible to analyze closely the effect of lacunarity on the universality classes. From Table V one can conclude that lacunarity strongly affects the ν exponent while its effect on the γ exponent is weaker. As a consequence, it is not possible to address any dependence of the exponent ν on D_f. In fact, our results also show that for lattices with the same D_f, when lacunarity decreases the ν exponent also decreases in contrast to previous works [2]. For a low-lacunarity carpet our result also suggest that ν has crossed over the two-dimensional value $\nu=1$.

We also display in Table V the average coordination number $\langle q\rangle$ [10] of each fractal lattice. From our results, there is a monotonic dependence of the critical parameter v_c on $\langle q\rangle$, but again there is no monotonic dependence of the critical exponents on $\langle q\rangle$. Earlier attempts [7] to address such dependence of the critical exponents with an effective dimension d' defined from the average number of bonds per site ($d'=\langle q\rangle/2$) did not include low-lacunarity carpets such as $(7,9)^l$ of Table V. Therefore, previous attempts [17] of interpreting the results for the critical exponents of the fractal lattices as arising from regular lattices at a noninteger effective dimension $d=d'$ or D_f were inconclusive. On the other hand, from our results, such a possible interpretation is not tenable.

Although all the lattices analyzed here have fractal dimension near 2, it is possible to apply the same technique to special Sierpinski carpets with D_f near 1 in which the lacunarity can be chosen to be arbitrarily small. Previous claims [18] that the critical behavior of the Ising model on such geometries become identical to those obtained from the analytic continuation of results for regular lattices with $D=1+\varepsilon$ could then be checked.

In Table VI we display, for comparison, the results obtained so far in the literature from several techniques for the carpet characterized by parameters $(b,m)=(3,1)$, $D_f=1.893$, and $d'=1.909$. We also include the critical exponents for Ising-like systems in regular lattices with noninteger dimension $d\simeq 1.9$ obtained from an ε-expansion technique for $d=2-\varepsilon$ [17].

TABLE V. Final estimates from first- and second-order approximants of the critical parameter v_c ($v_c=\tanh J/k_BT_c$) and exponents γ and ν for Sierpinski carpets characterized by parameters (b,m), average coordination number $\langle q\rangle$, and ordered according to their fractal dimension D_f. For comparison, the corresponding values for the 2D Ising model ($D_f=2$) are included. Asterisk denotes exact results: $v_c=0.4142\ldots$, $\gamma=1.75$, and $\nu=1$.

D_f	b,m	$\langle q\rangle$	v_c	γ	ν
			$K=1$ approximants		
2*		4	0.4142±0.0003	1.75±0.03	1.000±0.006
1.975	(5,1)	3.966	0.4201±0.0003	1.84±0.02	1.023±0.007
1.896	$(7,9)^l$	3.872	0.4521±0.0035	2.67±0.11	1.04±0.26
1.896	$(7,9)^h$	3.774	0.4687±0.0028	2.34±0.09	1.50±0.13
1.893	(3,1)	3.818	0.4560±0.0017	2.27±0.08	1.38±0.20
			$K=2$ approximants		
2*		4	0.4142±0.0002	1.753±0.016	1.000±0.008
1.975	(5,1)	3.966	0.4204±0.0005	1.86±0.03	1.035±0.039
1.896	$(7,9)^l$	3.872	0.4465±0.0069	2.38±0.32	0.83±0.23
1.896	$(7,9)^h$	3.774	0.4699±0.0053	2.49±0.31	1.36±0.21
1.893	(3,1)	3.818	0.4552±0.0015	2.24±0.12	1.38±0.16

TABLE VI. Results for the Sierpinski carpet $(b,m)=(3,1)$ obtained from several techniques. For comparison, the corresponding values for the Ising model on a regular lattice with effective dimension $d \simeq 1.9$ obtained from a ε-expansion method are included.

Method	T_c	γ	ν	β
16th-order series	2.034±0.006[a]	2.27±0.08[a]	1.38±0.16[a]	
9th-order series	2.07±0.02[b]	1.99±0.06[b]		
numerical	2.03±0.02[c]	1.980[c]	1.090[c]	0.0928[c]
simulations	2.09±0.03[d]	1.88±0.08[d]	1.09±0.05[d]	
RG	2.0631[e]			0.034[f]
	2.0619[g]		1.12[g]	
ε expansion				
$d \simeq 1.9$		1.862±0.015[h]	1.10±0.01[h]	0.097±0.003[h]

[a]Present work.
[b]Reference [8].
[c]Reference [6].
[d]Reference [7].
[e]Reference [3].
[f]Reference [4].
[g]Reference [5].
[h]Reference [17].

The series method used here gives results closer to the true values than previous estimates and may help to analyze the effect of the approximate methods used so far in the study of phase transitions on nontrivial fractals. In particular, the critical temperatures were obtained with high accuracy. In general, one can conclude that the critical temperatures in the RG schemes [3,5] compare well with our results, but the accuracy of the critical exponents, varies according to the self-similar factor of the lattice. On the other hand, Monte Carlo (MC) results [6,7] underestimate γ and ν, probably due to finite-size effects.

The finite-size effects in the MC simulations on fractals are stronger than in the Euclidean lattices because the full connectivity of the fractal lattices (or the correlation among the size distribution of the lacunas within the lattice) is not captured in the first stages of lattice construction, but only in an averaged way. Note that the proximity between the MC results and those for a homogeneous lattice with $d \simeq 1.9$ (see Table VI) also suggests this interpretation.

In our approach, we count exactly the density of each type of graph that contributes to (3) or (4) in the limit of infinite fractal lattice. Then the order propagation through the lattice is calculated including the existence of lacunas of all length scales, capturing the true critical behavior.

Previous high-temperature series results up to 9th order for the Ising magnetic susceptibility on carpets with central lacunas [8] overestimated T_c and underestimated γ. In fact, there is a change in the asymptotic series behavior near order 10 for all the analyzed fractals, which is also suggested by the appearance of a great number of D log Padé approximants with spurious poles. This shows that series expansions for fractals may exhibit a slow convergence and also that methods of series analysis other than D log Padé should be used to describe a more general critical behavior such as Eqs. (8) or (9).

The analysis of our series by first- and second-order differential approximants for the thermodynamic quantities of the Ising model on fractals with $1<D_f<2$ suggests the presence of analytic corrections to the leading singular behavior, analogously to the 2D systems. On the other hand, the existence of nonanalytic confluent singular terms is not ruled out, which may have not been captured numerically by this method. Other methods and longer series are needed to clear out this point.

The main result that arises from our calculations is that two critical leading exponents, namely, ν and γ, were obtained from series approach for Ising-like systems on nontrivial fractals. From them, other critical exponents follow, assuming the scaling relations for fractals. Applying the same method of graph counting one can also generate the high-temperature series expansion for the specific heat.

The technique used here is general and can be applied to a fairly large class of deterministic self-similar fractals. Systems on geometries with dimensions D_f arbitrarily close to any integer dimension D (including upper and lower critical dimensions) can be analyzed in a systematic way. Important open questions in the field of phase transitions such as the limiting behavior of critical exponents as $D_f \to D$ can now be addressed.

APPENDIX

Consider a particular Sierpinski carpet characterized by parameters b and m. Figure 1 gives examples of such fractals at the first stage of construction. The fractal at the lth stage of construction is formed by b^2-m reproductions of the previous $(l-1)$ stage with spatial distribution identical to the b^2-m subsquares left at the first stage.

The number of embeddings $G(l)$ of a particular graph in the lattice at stage l is given by

$$G(l)=(b^2-m)G(l-1)+H(l-1)\ , \tag{A1}$$

with

$$H(l-1)=H_1(l-1)+H_2(l-1)\ , \tag{A2}$$

where $H_1(l-1)$ and $H_2(l-1)$ represent the number of embeddings that cross, respectively, one and more than one intersection between the reproductions of the $(l-1)$

stage at the lth lattice stage.

Now, for this particular graph, consider the minimal stage l_0 that embeds it and proceed as follows.

(a) Compute exactly the total number of possible embeddings of the graph at stage l_0. This gives $G(l_0)$.

(b) Consider two neighboring l_0 stage reproductions and compute the total number of possible embeddings that cross the intersection between them. This number times the number of such pairs in the next scale gives $H_1(l_0)$.

(c) Consider three or four neighboring l_0 stage reproductions (see Fig. 2) and compute the total number of possible embeddings that cross two or more intersections between them. By considering all possible sets of such l_0 scale reproductions in the next scale, obtain $H_2(l_0)$.

It is possible to show that [9]

$$H_1(l-1)=bH_1(l-2)+(b-1)C_1 \tag{A3}$$

and

$$H_2(l-1)=H_2(l_0)=C_2 , \tag{A4}$$

where C_1 and C_2 depend only on the embedding properties of the graph at stage l_0 and the geometric properties of the initiator of the fractal. The first term on the right-hand side of Eq. (A3) comes from [9] the b reproductions of scale $(l-2)$ that are close to each lateral border of the scale $(l-1)$.

Iterating (A3) up to scale l_0 and adding the result to (A4):

$$H(l-1)=C_3b^{l-1}+C_4 , \tag{A5}$$

where C_3 and C_4 depend on $H_1(l_0)$, C_1, and C_2.

Substituting (A5) in (A1) and iterating up to l_0, we obtain

$$G(l)=A(b^2-m)^l+Bb^l+C , \tag{A6}$$

with constants A, B, and C obtained from geometric properties of the initiator and embedding properties of the graph at the stage l_0 $[C_1,H_1(l_0),H_2(l_0),G(l_0)]$.

In particular, Eq. (A6) is also valid for the number of sites $N(l)$ at each stage l (with constants A', B', and C').

The density of a particular graph in the infinite fractal lattice is then

$$g=\lim_{l\to\infty}\frac{G(l)}{N(l)}=\frac{A}{A'} . \tag{A7}$$

From (A7) it is possible to obtain the exact evaluation of the nth order of the series by considering all the contributions of graphs with n bonds.

To illustrate, we give the results for the particular graph shown in Fig. 2 on the carpet with $b=3$ and $m=1$. The graph is a self-avoiding chain with five bonds and contributes with weight 16 for the 5th order of series (3) and (4). In this case, $l_0=1$ and $G(l_0)=2$ (see Fig. 3). In Fig. 4 we show the possible five embeddings that cross one intersection between two neighbor l_0 scale reproductions. There are four intersections of this sort in the next scale of the lattice (corresponding to four horizontal or vertical bonds between the remaining subsquares of the initiator of the carpet). This gives $H_1(l_0)=20$.

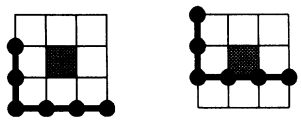

FIG. 3. Contributions to $G(l_0)=2$ of the particular example at minimum stage $l_0=1$ of the fractal lattice with $b=3$ and $m=1$.

The constant C_1 in (A3) represents particular embeddings that cross two neighbor general $(l-1)$ stage reproductions which can be computed by considering only neighbor l_0 stage reproductions (see Ref. [9]). Figure 5 shows the four possible embeddings in the case of our example. By considering the four similar intersections (horizontal or vertical) of the $(l-1)$ stage at the lth stage, we obtain $C_1=16$.

Finally, the $H_2(l_0)=6$ embeddings are shown in Fig. 6. (For this particular fractal there are sets of only three neighbor $(l-1)$ stage reproductions in the lth stage).

Iterating (A3) [using $H_1(l_0)=20$ and $C_1=16$] and adding (A4) [$H_2(l_0)=6$], we get for this particular graph in the particular fractal with $b=3$ and $m=1$

$$H(l-1)=12\times3^{l-1}-10 . \tag{A8}$$

Then (A1) reads

$$G(l)=8G(l-1)+12\times3^{l-1}-10 . \tag{A9}$$

Iterating (A9) up to l_0 and using $G(l_0)=2$, we finally get

$$G(l)=\tfrac{34}{35}8^l-\tfrac{12}{5}3^l+\tfrac{10}{7} . \tag{A10}$$

Now we show explicitly the calculation of the number of embeddings in the carpet with $b=3$ and $m=1$ at stage l of two special graphs: the number of sites (graphs of length 0) $N(l)$ and the number of bonds (graphs of length 1, horizontal and vertical) $L(l)$. First, note that $H(l-1)$ in (A1) is zero for both graphs. On the other hand, sites

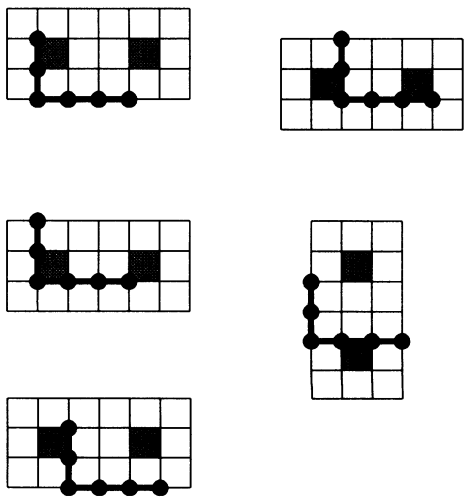

FIG. 4. The five distinct ways of embedding the graph crossing two neighbor l_0-stage reproductions.

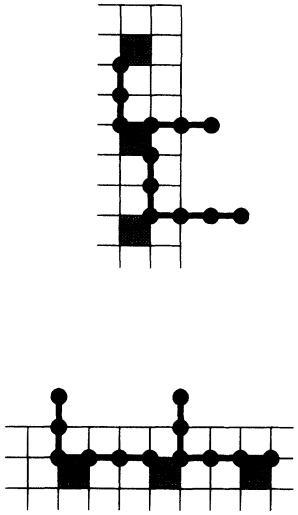

FIG. 5. The four distinct embeddings that contributes to constant C_1 in Eq. (A3) for this particular graph.

and bonds that belong to the common border of two adjacent reproductions of stage $(l-1)$ at stage l are counted twice in (A1). There are $3^{l-1}+1$ sites and 3^{l-1} bonds at each lateral border of the carpet ($b=3$) at stage $(l-1)$. Also, there are eight borders shared by two adjacent $(l-1)$ stage reproductions in the stage l (corresponding to eight horizontal and vertical bonds between the remaining subsquares of the initiator of the carpet). Then, including a correction term in (A1) for $N(l)$ and $L(l)$, we get ($b=3$, $m=1$, and $b^2-m=8$)

$$N(l)=8N(l-1)-8(3^{l-1}+1) \tag{A11}$$

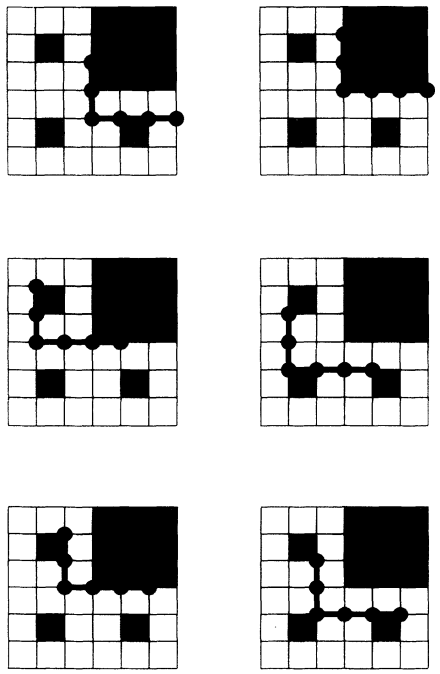

FIG. 6. Illustration of the $H_2(l_0)=6$ embeddings of the graph.

FIG. 7. Graphs that contribute to the second order of the series given by Eqs. (3b) and (4): (a) graph 1 and (b) graph 2.

and

$$L(l)=8L(l-1)-8\times 3^{l-1}\ . \tag{A12}$$

Iterating (A11) and (A12) up to $l_0=1$ and using $N(1)=16$ and $L(1)=24$, we obtain

$$N(l)=\tfrac{44}{35}8^l+\tfrac{8}{5}3^l+\tfrac{8}{7} \tag{A13}$$

and

$$L(l)=\tfrac{12}{5}8^l+\tfrac{8}{5}3^l\ . \tag{A14}$$

From (A7), and using (A13) and (A14), we get the coefficients of the first order d_1 in (3b) and ρ_1 in (5) for the carpet with $b=3$ and $m=1$. The weight for each bond is 2 and the end-to-end distance $r=1$. Thus

$$\rho_1=d_1=\lim_{l\to\infty}\frac{2L(l)}{N(l)}=\frac{42}{11}\ , \tag{A15}$$

as shown in Tables I and II.

The coefficients d_2 and ρ_2 for the carpet with $b=3$ and $m=1$ can also be easily calculated. The graphs that contribute to the second order of series (3b) and (4) are shown in Fig. 7 and numbered as 1 and 2, respectively. In Table VII we show the constants that appear in (A1)–(A6) for both graphs.

For graph 2, the data in Table VII lead directly to the number of embeddings in stage l:

$$G_2^{(2)}(l)=\tfrac{8}{7}8^l-\tfrac{1}{7}\ . \tag{A16}$$

However, for graph 1 (as well as for any other graph with bonds in a unique direction), the embeddings at the borders of two adjacent reproductions of stage $(l-1)$ in the stage l are counted twice in (A1) (there are $3^{l-1}-1$ embeddings of this sort at each border). The same occurs for the embeddings located along the borders of each two adjacent reproductions of stage $(l-2)$ in stage $(l-1)$ represented by the first term on the right-hand side of Eq. (A3) [there are 2 (or $b-1$) embeddings of this sort; see Ref. [9]].

By considering the four similar borders (horizontal or vertical) of the $(l-1)$ stage at the lth stage, Eqs. (A1) and (A3) for graph 1 (including the correction terms) are rewritten as ($b=3$, $m=1$, and $b^2-1=8$)

$$G(l)=8G(l-1)+H(l-1)-4(3^{(l-1)}-1) \tag{A17}$$

TABLE VII. Constants appearing in Eqs. (A1)–(A6) for graphs 1 and 2 that contributes to the second order of the series (see text).

Graph	$G(l_0)$	$H_1(l_0)$	C_1	$H_2(l_0)$
1	8	16	0	0
2	9	0	0	1

FIG. 8. Graphs that contribute to the third order of the series given by Eqs. (3b) and (4): (a) graph 1, (b) graph 2, (c) graph 3, and (d) graph 4.

and

$$H_1(l-1)=3H_1(l-2)+2C_1-4\times 2\ . \tag{A18}$$

Using the data in Table VII, we get, for the number of embeddings of graph 1 in stage l,

$$G_2^{(1)}(l)=\tfrac{8}{7}8^l-\tfrac{8}{7}\ . \tag{A19}$$

Graphs 1 and 2 (see Fig. 7) have, respectively, weights 4 and 8 and end-to-end distances $r=2$ and $\sqrt{2}$. Using (A7) and (A13), from (A16) and (A19) we get

$$d_2=\frac{4\times\frac{8}{7}+8\times\frac{8}{7}}{\frac{44}{35}}=\frac{120}{11} \tag{A20}$$

and

$$\rho_2=\frac{4\times\frac{8}{7}\times 4+8\times\frac{8}{7}\times 2}{\frac{44}{35}}=\frac{320}{11}\ , \tag{A21}$$

as shown in Tables I and II.

The graphs that contribute to the third order of the series are shown in Fig. 8 and numbered as 1–4. Their embeddings in stage l of carpet $(b,m)=(3,1)$ are obtained with the same techniques used to get Eqs. (A10), (A16), and (A19):

$$G_3^{(1)}(l)=\tfrac{38}{35}8^l-\tfrac{4}{5}3^l-\tfrac{16}{7}\ , \tag{A22a}$$

$$G_3^{(2)}(l)=\tfrac{38}{35}8^l-\tfrac{4}{5}3^l-\tfrac{2}{7}\ , \tag{A22b}$$

$$G_3^{(3)}(l)=\tfrac{38}{35}8^l-\tfrac{4}{5}3^l-\tfrac{2}{7}\ , \tag{A22c}$$

$$G_3^{(4)}(l)=\tfrac{9}{8}8^l\ . \tag{A22d}$$

The respective weights are 4, 16, 8, and 8. The reader can easily check coefficients d_3 and ρ_3 in Tables I and II.

[1] B. B. Mandelbrot, in *The Fractal Geometry of Nature* (Freeman, San Francisco, 1982).
[2] Y. Gefen, A. Aharony, and B. B. Mandelbrot, J. Phys. A **17**, 1277 (1984); R. Riera and C. M. Chaves, Z. Phys. B **62**, 387 (1985); Y. K. Wu and B. Hu, Phys. Rev. A **35**, 1404 (1987).
[3] U. M. S. Costa, I. Roditi, and E. M. F. Curado, J. Phys. A **20**, 6001 (1987).
[4] A. Chame and U. M. S. Costa, J. Phys. A **23**, L1127 (1990).
[5] B. Bonnier, Y. Leroyer, and C. Meyers, Phys. Rev. B **37**, 5205 (1988).
[6] J. C. Angles d'Auriac and R. Rammal, J. Phys. A **19**, L655 (1986).
[7] B. Bonnier, Y. Leroyer, and C. Meyers, J. Phys. (Paris) **48**, 553 (1987).
[8] B. Bonnier, Y. Leroyer, and C. Meyers, Phys. Rev. B **40**, 8961 (1989).
[9] Fábio D. A. Aarão Reis and R. Riera, Phys. Rev. A **45**, 2628 (1992).
[10] Fábio D. A. Aarão Reis and R. Riera, J. Stat. Phys. **71**, 467 (1993).
[11] C. Domb, in *Phase Transitions and Critical Phenomena*, edited by C. Domb and M. S. Green (Academic, London, 1974), Vol. 3.
[12] M. E. Fisher and R. J. Burford, Phys. Rev. **156**, 583 (1967).
[13] A. J. Guttmann, J. Phys. A **20**, 1839 (1987).
[14] J. J. Rehr, G. S. Joyce, and A. J. Guttmann, J. Phys. A **13**, 1587 (1980).
[15] A. Aharony and M. E. Fisher, Phys. Rev. Lett. **45**, 679 (1980).
[16] A. J. Liu and M. E. Fisher, Physica A **156**, 35 (1989).
[17] J. C. Le Guillou and Z. Zinn-Justin, J. Phys. (Paris) **48**, 19 (1987).
[18] Y. Gefen, Y. Meir, B. B. Mandelbrot, and A. Aharony, Phys. Rev. Lett. **50**, 145 (1983).

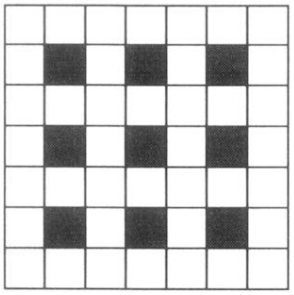

(a)

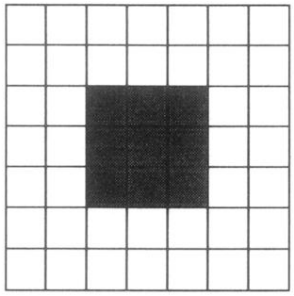

(b)

FIG. 1. Initiators of Sierpinski carpets characterized by parameters $b=7$ and $m=9$: (a) high lacunarity and (b) low lacunarity.

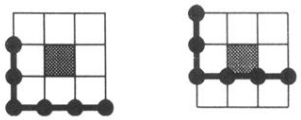

FIG. 3. Contributions to $G(l_0)=2$ of the particular example at minimum stage $l_0=1$ of the fractal lattice with $b=3$ and $m=1$.

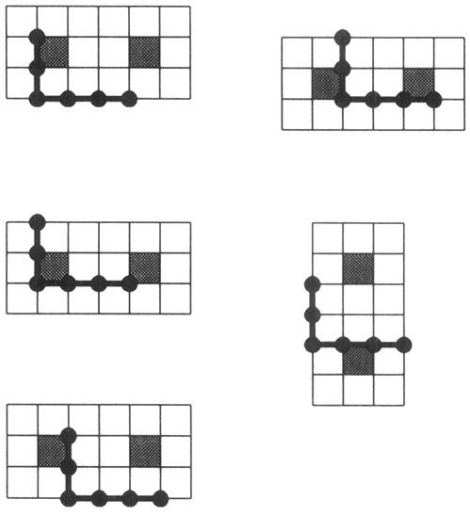

FIG. 4. The five distinct ways of embedding the graph crossing two neighbor l_0-stage reproductions.

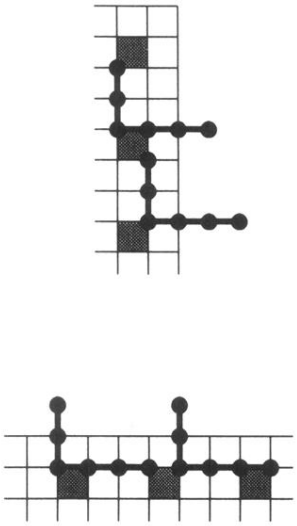

FIG. 5. The four distinct embeddings that contributes to constant C_1 in Eq. (A3) for this particular graph.

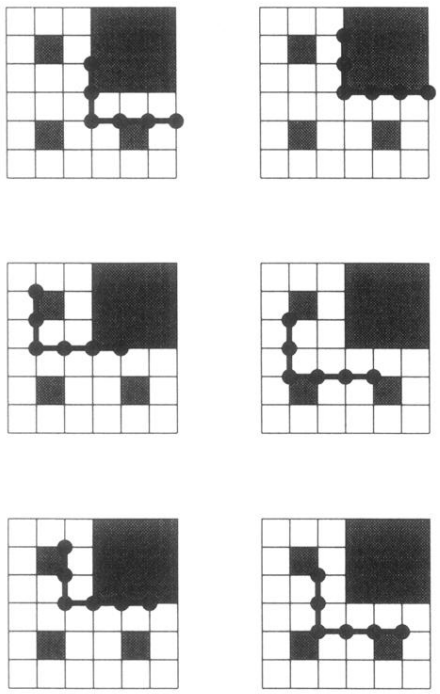

FIG. 6. Illustration of the $H_2(l_0)=6$ embeddings of the graph.